

Energy Flux and Bottleneck Effect in Turbulence

Mahendra K. Verma

Department of Physics, Indian Institute of Technology, Kanpur 208016, India

Diego Donzis

Georgia Institute of Technology, School of Aerospace Engineering, Atlanta, GA 30332, USA

Past numerical simulations and experiments of turbulence show bottleneck effect. In this paper we show that sufficiently large inertial range (more than two decades) is required for an effective energy cascade. The bottleneck effect is due to insufficient inertial range in simulations and experiments. To compensate, the spectrum near Kolmogorov's dissipation wavenumber has a hump. Data from numerical simulations in literature show that the bottleneck effect is enhanced by hyperviscosity; we argue that this effect is because of decrease in the dissipation range due to hyperviscosity.

INTRODUCTION

Energy spectrum of turbulent flow is an important quantity. In 1941, Kolmogorov [1] showed that the energy spectrum $E(k)$ of turbulent flow is

$$E(k) = K_{K_0}^{-2/3} k^{-5/3} f(k=k_d); \quad (1)$$

where E is the energy flux, K_{K_0} is Kolmogorov's constant, k_d is Kolmogorov's wavenumber, and the function $f(x) \approx 1$ in the inertial range ($x \approx 1$), and $f(x) \approx 0$ as $x \gg 1$. Many experiments and numerical simulations verify this powerlaw apart from a very small intermittency correction. The normalized energy spectrum $E(k)k^{5/3}=K_{K_0}$ is flat in the inertial range, and decays in the dissipation range. Careful observation of recent high resolution numerical simulation [2, 3] and experiments [4, 5] however show a small hump in the normalized energy spectrum near Kolmogorov's wavenumber k_d . The feature is called "bottleneck effect" in literature. In this paper we propose an explanation for the bottleneck effect.

Saddoughi and Veeravalli [5] studied the energy spectrum of atmospheric turbulence and observed bottleneck effect. They found that the longitudinal spectra has larger inertial range (around 1.5 decade) but smaller hump, while the transverse spectra has relatively smaller inertial range (around one decade), but larger hump. Bottleneck effect has been observed in other experiments as well, for example by Pak et al. [4, 6]. Many high resolution simulations also show the bottleneck effect. Kaneda et al. [7], and Dobler et al. [3] found bottleneck effect in fluid turbulence, Watanabe and Gotoh and others [8, 9, 10] in scalar turbulence, Haugen et al. [11] in three-dimensional magnetohydrodynamics, Biskamp et al. [12] in two-dimensional magnetohydrodynamics, electron-magnetohydrodynamics, and thermal convection. Lamorgese et al. [13], Biskamp et al. [12], and Dobler et al. [3] observed that the bottleneck effect become more pronounced when hyperviscosity is increased.

To explain bottleneck effect theoretically, Yakhot and Zakharov [14] derived energy spectrum using Clebsch variables and showed that the energy spectrum is

$$E(k) = K_{K_0}^{-2/3} k^{-5/3} f(k=k_d) + P k^{-1}; \quad (2)$$

i. e., correction is of the form k^{-1} . Theoretical justification for k^{-1} was argued by Orszag [15] who analyzed the one-loop Dyson equation for the propagator G and the velocity correlation function U . The spectrum k^{-1} was obtained by assuming that the response function is dominated by viscous effects. Falkovich [16] argued that the viscous suppression of small-scale modes removes some triads from nonlinear interactions, thus making it less effective, which leads to pileup of energy in the inertial interval of scales. For quantitative explanation, Falkovich applied perturbative technique used in wave turbulence and derived the following formula for the correction in Kolmogorov's spectrum:

$$E(k) = E(k) (k=k_p)^{4/3} = \ln(k_p=k); \quad (3)$$

where k_p is proportional to the dissipative wavenumber k_d . The above formula is valid for $k \gg k_p$. Our theoretical idea has certain similarity with that of Falkovich; the theoretical predictions however are quite different as described below.

THE REASON FOR THE BOTTLENECK EFFECT

The basic idea presented in our paper is as follows: In a fully-developed turbulence, a flux of energy is transferred from small wavenumbers to large wavenumbers. This process involves interactions of large number of modes — from small wavenumbers to large wavenumbers. The energy transfer between wavenumber shells is local, i. e., from a given shell, the maximum amount of energy is transferred to its nearest neighbour shell. Still significant energy transfer takes place between somewhat distant wavenumber shells [17, 18, 19, 20, 21, 22]. Verma et al. [22] showed using a theoretical arguments that if the inertial range shells are divided in such a way that the m th shell is given by $k_0 (2^{m-4} : 2^{(m+1)-4})$, then in the inertial-range the normalized shell-to-shell energy transfer rates from shell m to shell $m+1; m+2; m+3$ are 18%; 6.7%; and 3.6% respectively. This result is in agreement with simulation results [22].

The above arguments imply that for effective cascade of energy, there must be large enough range of wavenumbers. Ideally, when Kolmogorov's wavenumber $k_d = 1$, Kolmogorov's cascade is setup, and the energy spectrum is given by Eq. (1). However, if Kolmogorov's wavenumber is not sufficiently large, and if we still supply the same amount of energy at large scale, the cascade process faces difficulty; at higher wavenumbers there are not enough number of modes to receive the energy transferred from the smaller wavenumbers. To compensate, the wavenumbers near Kolmogorov's scale have higher energy level. This is the basic reason for the bottleneck effect. Note that the energy fed at the small wavenumber fixes the level of energy spectrum in the inertial range, and the energy input has to be dissipated at the higher wavenumbers. In the following discussion we will present a quantitative arguments to support the above idea.

Formalism

The average energy flux from a wavenumber sphere of radius k_0 is given by [23, 24, 25]

$$\langle k_0 \rangle = \frac{1}{Z} \int_{k > k_0} dk \int_{p < k_0} dp \, hS(k \cdot p \cdot q) i \quad (4)$$

where $S(k \cdot p \cdot q)$ is the “mode-to-mode energy transfer rate” in a triad (p, q, k) with $k = p + q$, and hS represents the ensemble average. The term $S(k \cdot p \cdot q)$ represents the energy transfer rate from mode p to mode k with mode q acting as a mediator. The term $hS(k \cdot p \cdot q)i$ has been earlier computed perturbatively using standard field-theoretic technique or eddy-damped quasi-normal Markovian approximation (EDQNM) [23, 24, 25]. The procedure to compute $\langle k_0 \rangle$ are described in Leslie [24] and Lesieur [23]. Here we give the formula presented in Verma [25]:

$$\langle k_0 \rangle = K_{K_0}^{3=2} \int_{k_0}^{\infty} dk \int_0^{k_0} dp \int_{k-p}^{k+p} dq \frac{pq T_1 C(p) C(q) + T_2 C(q) C(k) + T_3 C(p) C(k)}{4k (k^{2=3} + p^{2=3} + q^{2=3})} ; \quad (5)$$

where K_{K_0} is the renormalized parameter [25, 26]. The correlation function $C(k)$ is related to the one-dimensional energy spectrum $E(k)$:

$$C(k) = \frac{E(k)}{4 k^2} ; \quad (6)$$

and

$$\begin{aligned} T_1 &= kp(xy + 2z^3 + 2xyz^2 + x^2z); \\ T_2 &= kp(xy + 2z^3 + 2xyz^2 + y^2z); \\ T_3 &= kq(xz - 2x\dot{y}z - \dot{y}^2z); \end{aligned}$$

where x, y, z are cosines defined as

$$p \cdot q = p q x; \quad q \cdot k = q k y; \quad p \cdot k = p k z;$$

Energy Spectrum

In this subsection we will compute flux by substituting a model energy spectrum for realistic turbulent flow, and energy spectrum from direct numerical simulations (DNS) in Eq. (5). The energy spectrum for realistic turbulent

flows is typically modelled as

$$E(k) = K_{K_0} A(k=k_f) \cdot k^{2=3} \cdot k^{5=3} \exp(-ck=k_d); \quad (7)$$

where

$$A(x) = \frac{x^{s+5=3}}{1+x^{s+5=3}} \quad (8)$$

with forcing wavenumber $k_f = 2$, $c = (0.2; 1.0)$, and $s = 4$. We take $K_{K_0} = 1.58$ [23, 25] throughout this paper. Clearly, $E(k) \propto k^s$ for $k < k_f$, $E(k) \propto k^{5=3}$ for the intermediate range, and $E(k) \propto k^{5=3} \exp(-ck=k_d)$ for the dissipation range. Note that an inclusion of hyperviscosity dampens the dissipative range strongly. The values of $c = 0.2; 1.0$ are chosen to model ordinary viscosity and hyperviscosity respectively.

Without loss of generality we can take $s = 1$ and study the energy fluxes for $k_d = 10^3; 10^4$ and 10^5 . In Fig. 1 we plot the compensated energy spectrum

$$E(k) = E(k)k^{5=3} = K_{K_0} = A(k=k_f) \exp(-ck=k_d) \quad (9)$$

As expected, higher k_d produces a larger inertial range. In hyperviscous case ($k_d = 10^4; c = 1.0$) the spectrum drops more sharply as compared to viscous case ($k_d = 10^4; c = 0.2$).

We compare our theoretical results with numerical simulation, which are performed for homogeneous, isotropic turbulence with stochastic forcing at low wavenumbers. These simulations were done at 512^3 , 1024^3 , and 2048^3 grids. Taylor-based Reynolds numbers for these runs were approximately 240, 400 and 700 respectively. Please refer to Yeung et al. [10] for details on simulations. We multiply the numerical energy spectrum with $k^{5=3} = K_{K_0}$ ($K_{K_0} = 1.58$), and then divide the resultant quantity by its maximum value, and obtain compensated energy spectrum. In the inertial range, the value of compensated energy spectrum is 1, hence the energy flux (or the energy input at small wavenumber) is $K_{K_0}^{3=2}$. In Fig. 1 we plot compensated energy spectra for DNS at 512^3 , 1024^3 , and 2048^3 grids. The hump appears in all the DNS plots indicating existence of bottleneck effect in numerical simulations.

Comparison of energy spectra for different grid resolutions reveals that the hump is most dominant for 512^3 , and it decreases as the grid size is increased, a phenomena observed in earlier numerical results as well. This result indicates the the bottleneck effect decreases with the increase of inertial range, thus reinforcing our hypothesis that the bottleneck effect is due to nonavailability of sufficient range of wavenumbers to facilitate energy cascade. In the following discussion we will revisit this hypothesis in view of energy flux.

Energy flux

We return to Eq. (5) and substitute $s = 1$. We compute the integral $I(k_0)$ (the bracketed term of Eq. [5]) for various values of k_d . When $k_d = 1$ and $A(x) = 1$, the integral $I_1 = 0.503$ independent of k_0 , implying that the flux is is independent of k_0 for the Kolmogorov energy spectrum ($E(k) = K_{K_0} \cdot k^{2=3} \cdot k^{5=3}$). Using I_1 we find the Kolmogorov constant, $K_{K_0} = 1.58$.

Now we compute the integral $I(k_0)$ using the model spectrum with $s = 4$ and $(k_d; c) = (100; 0.2); (1000; 0.2); (10000; 0.2)$. The value of $I(k_0)$ starts from 0 at $k_0 = 0$, reaches a peak, and then it decays. We compute the values of energy fluxes at various wavenumbers using

$$(k_0) = K_{K_0}^{3=2} I(k_0) \quad (10)$$

with $K_{K_0} = 1.58$. Fig. 2 contains plots of (k_0) vs. k_0 for different values of $(k_d; c)$. The maximum values of (k_0) for these cases are listed in Table 1. They are all less than 1, with the difference from the actual value (1) increasesing with the decrease k_d . Theoretically $\max((k_0))$ must be 1 because the energy input at the small wavenumber is 1. *The reason for the decrease in $\max((k_0))$ is the lack of modes in the large wavenumber region. The viscous suppression of large-wavenumber modes removes these modes.* This is where the hump in the energy spectrum near dissipation wavenumber comes into play.

We compute the flux integral using the compensated energy spectra $E(k)$ obtained from DNS at 512^3 , 1024^3 , and 2048^3 grids, and compute $\max((_{DNS})$. These values are listed in Table 1. The value of $\max((_{DNS})$ for 2048^3 is very close to unity. Clearly the energy spectra obtained from numerical simulations provide a better handle on energy flux as compared to the model energy spectrum [Eq. (7)]. This is because of the higher level of energy spectrum (hump) near Kolmogorov's wavenumber in the DNS (see Fig. 1), which makes up for the loss of large wavenumber modes.

The overall effect is that the energy flux in high-resolution DNS is close to what we would get in idealized situation when $k_d \gg 1$. Thus consistency with Kolmogorov's theory is achieved. The value $m_{\max} (_{\text{DNS}})$ for 512^3 is somewhat higher than 1, which may be due to approximations made in our theoretical calculations.

Required range of inertial range to nullify bottleneck

Verma et al. [22] and Verma [25] computed the shell-to-shell energy transfer rate from m th wavenumber shell to n th wavenumber shell (T_n^m) using

$$T_n^m = K_{K_0}^{3=2} \int_{k_2 s_n}^{Z} \int_{p_2 s_m}^{Z} \int_{jk pj}^{Z_{k+p}} \frac{dp dq}{4k} \frac{pq T_1 C(p) C(q) + T_2 C(q) C(k) + T_3 C(p) C(k)}{(k^{2=3} + p^{2=3} + q^{2=3})} ; \quad (11)$$

where s_m, s_n are the wavenumber range for the m th and n th shell respectively. The wavenumber space is divided into various shells logarithmically. In Verma et al. [22] and Verma [25] the m th shell is ($2^{m=4} : 2^{(m+1)=4}$).

Verma et al. [22] and Verma [25] computed T_n^m in the inertial range using a similar procedure as described in the previous subsection. Kolmogorov's spectrum $k^{5=3}$ was assumed throughout the wavenumber space. They found that maximum energy transfer takes place to the nearest neighbour, yet significant energy is transferred to other shells. For example, the energy transfer rate from m th shell to the shells $m+1, m+2$, and $m+3$ are 18%, 6.7%, and 3.6% respectively. The transfer rate decreases monotonically for more distant shells.

Let us imagine a wavenumber sphere of radius R . Using the shell-to-shell energy transfer rates we can compute the energy transfers from the above wavenumber sphere to n shells adjacent to the sphere (wavenumber range: $R : R : 2^{=4}$). Simple algebra shows that the above quantity is [25]

$$\frac{Q_n}{m=1} = \frac{X^n}{m} : \quad (12)$$

In Table 2 we list Q_n for various values of n . The Table shows that 42.2% of the flux is transferred to the three adjacent shells. *To transfer 99.1% energy we need 28 shells.* Clearly, we need large number of wavenumber shells for effective energy transfer. This is the reason for the bottleneck effect when inertial range is short. Bottleneck disappears when there are sufficient wavenumber shells to complete the energy transfer.

In the following discussion we estimate the required length of inertial range to nullify bottleneck effect. We take a flux-sphere of radius R in the inertial range, then, as argued in the previous paragraph, for effective energy transfer the last wavenumber of the inertial range has to be at least $R : 2^{28=4}$. Using these numbers the crude estimate of required inertial range is $k_{\max} = R = 2^7$ to $k_{\max} = 2^7 R$, or $k_{\max} = k_{\min} : 2^8 = 256$. Hence the inertial range wavenumbers must be more than two decades. The current numerical simulations have inertial range lower than these values, hence they exhibit bottleneck effects. The experimental spectra reported by Saddoughi and Veeravalli [5] too have inertial range less than two decades, and they show strong bottleneck effect. The energy spectra plots of Fig. (1) shows that only kd10000 run, which has negligible bottleneck effect, has inertial range more than two decades. Hence current numerical and experimental results are in agreement with the above estimate of wavenumber-range for nullifying the bottleneck effect.

Effects of hyperviscosity

Lamorgese et al. [13], Biskamp et al. [12], and Dobler et al. [3] have reported that hyperviscosity increases the bottleneck effect. It appears counter-intuitive because hyperviscosity increases the inertial range, so it must decrease bottleneck effect. We carried out energy flux calculations for ($k_d = 10^4; c = 0.2$) and ($k_d = 10^4; c = 1.0$). Loosely speaking, the former corresponds to ordinary viscosity and the latter corresponds to hyperviscosity. As shown in Fig. 2 and Table 1, the flux for the latter is lower than that for the former. *This is because of lack of sufficient number of modes in the dissipative range for the hyperviscous case.* We believe the enhanced bottleneck effect with hyperviscosity is due to decrease in dissipation range. Note that this argument differs from ones described in previous subsections where bottleneck effect is related to the decrease in inertial range.

CONCLUSIONS

To summarize, in this paper we investigated the reason for bottleneck effect in turbulence. The energy is supplied at large scales, and it cascades to smaller scales. Even though most energy goes to the next wavenumber shells, there is a significant energy transfers to far-away wavenumber shells. We showed that effective transfer of energy flux in the inertial range can take place when there is at least two decades of inertial range. If the inertial range is shorter, a hump is created near Kolmogorov's scale (beginning of dissipation range) which compensates for the nonexistence of required inertial range. This phenomena is seen in all the current numerical simulations, and some experiments which do not have at least two decades of inertial range.

Yakhot and Zakharov [14] and Falkovich [16] derived the corrections in the energy spectrum due to bottleneck effect [see Eqs. (2, 3)]. In the present paper we do not the address the form of correction in energy spectrum. Rather, we show using flux analysis that Kolmogorov's spectrum with short inertial range exhibits bottleneck effect. Hence, our results complement Yakhot and Zakharov [14] and Falkovich [16] findings. Note however that the predictions of Yakhot and Zakharov, and Falkovich are not the same, and they need to be tested carefully.

The energy transfer in turbulence of passive scalar follows similar patterns as in fluid turbulence. Hence bottleneck effect is expected in scalar turbulence as well. This has been verified by Watanabe and Gotoh [8] and Yeung et al. [9, 10], who observed strong bottleneck effect in their simulations of passive-scalar turbulence. In three-dimensional magnetohydrodynamics too, energy transfer is forward and local, yet significant range of inertial-range is required for effective energy transfer [27]. Therefore, bottleneck effect is expected in magnetohydrodynamics turbulence; the numerical results of Haugen et al. [11] are consistent with this hypothesis. The bottleneck effects has been observed in electron-magnetohydrodynamic (EMHD) turbulence, and two-dimensional turbulence (see Biskamp et al. [12] and references therein), but their cause is possibly more complex. It has been observed that the bottleneck effect along the transverse and longitudinal directions are different [5]; this result still lacks satisfactory explanation. Future developments in theoretical turbulence will possibly resolve some of these issues.

We gratefully acknowledge useful discussions with K. R. Sreenivasan and P. K. Yeung, and hospitality of International Center for Theoretical Physics (ICTP), Trieste, during our visit in Summer 2005 when part of this work was done. We thank P. K. Yeung for sharing the numerical data with us. The simulations used in this work were done at the San Diego Supercomputer Center and the National Energy Research Scientific Computing Center.

[1] A. N. Kolmogorov, *Dokl. Akad. Nauk SSSR* **30**, 9 (1941).

[2] Z. S. She, S. Chen, G. Doolen, R. H. Kraichnan, and S. A. Orszag, *Phys. Rev. Lett.* **70**, 3251 (1993).

[3] W. Dobler, N. E. L. Haugen, T. A. Yousef, and A. Brandenburg, *Phys. Rev. E* **68**, 26304 (2003).

[4] Z. S. She and E. Jackson, *Phys. Fluids A* **5**, 1526 (1993).

[5] S. G. Saddoughi and S. V. Veeravalli, *J. Fluid Mech.* **268**, 333 (1994).

[6] H. K. Pak, W. I. Goldburg, and A. Sirivat, *Fluid Dyn. Res.* **8**, 19 (1991).

[7] Y. Kaneda, T. Ishihara, M. Yokokawa, K. Itakura, and A. Uno, *Phys. Fluids* **15**, L21 (2003).

[8] T. Watanabe and T. Gotoh, *New Journal of Physics* **6**, 40 (2004).

[9] P. K. Yeung, *J. Fluid Mech.* **321**, 235 (1996).

[10] P. K. Yeung, D. A. Donzis, and K. R. Sreenivasan, *Phys. Fluids* **17**, 81703 (2005).

[11] N. E. L. Haugen, A. Brandenburg, and W. Dobler, *Phys. Rev. E* **70**, 16308 (2004).

[12] D. Biskamp, E. Schwarz, and A. Celani, *Phys. Rev. Lett.* **14**, 4855 (1998).

[13] A. G. Lamorgese, D. A. Caughey, and S. B. Pope, *Phys. Fluids* **17**, 15106 (2005).

[14] V. Yakhot and V. Zakharov, *Physica D* **64**, 379 (1993).

[15] S. A. Orszag, in *Fluid Dynamics, Les Houches 1973 Summer School of Theoretical Physics* (Gordon and Breach, Berlin, 1977), p. 273.

[16] G. Falkovich, *Phys. Fluids* **6**, 1411 (1994).

[17] R. H. Kraichnan, *J. Fluid Mech.* **47**, 525 (1971).

[18] Y. Zhou, *Phys. Fluids* **5**, 1092 (1993).

[19] Y. Zhou and C. G. Speziale, *Appl. Mech. Rev.* **51**, 267 (1998).

[20] J. A. Domaradzki and R. S. Rogallo, *Phys. Fluids A* **2**, 413 (1990).

[21] F. Waleffe, *Phys. Fluids A* **4**, 350 (1992).

[22] M. K. Verma, A. Ayyer, O. Debliquy, S. Kumar, and A. V. Chandra, *Pramana, J. Phys.* **65**, 297 (2005).

[23] M. Lesieur, *Turbulence in Fluids - Stochastic and Numerical Modelling* (Kluwer Academic Publishers, Dordrecht, 1990).

[24] D. C. Leslie, *Development in the Theory of Turbulence* (Oxford University Press, Clarendon, 1973).

[25] M. K. Verma, *Phys. Rep.* **401**, 229 (2004).

[26] M. K. Verma, *Phys. Plasmas* **8**, 3945 (2001).

[27] M. K. Verma, A. Ayyer, and A. V. Chandra, Phys. Plasmas **12**, 82307 (2005).

Table I: The maximum values of energy fluxes for the model energy spectra [Eq. (7)] with $(k_d; c) = (100; 0.2); (1000; 0.2); (10000; 0.2); (10000; 1)$ and for energy spectra obtained from numerical simulations on $512^3; 1024^3$ and 2048^3 grids. $c = 1.0$ and $c = 0.2$ correspond to hyperviscosity and ordinary viscosity respectively. For Kolmogorov's spectrum $\max(k_0) = 1$.

	k_d	$\max(k_0)$
kd100	100	0.84
kd1000	1000	0.94
kd10000	10000	0.96
hyper	10000	0.928
DNS512	-	1.14
DNS1024	-	1.09
DNS2048	-	1.02

Table II: The energy transfer rates from a wavenumber sphere in the inertial range to n shells adjacent to the sphere $Q_n = \sum_{m=1}^n T_n^m$ for various n 's.

n	1	2	3	8	28	32	48
$2^{n=4}$	$2^{1=4}$	$2^{1=2}$	$2^{3=4}$	4	128	256	4098
$Q_n =$	0.184	0.316	0.422	0.739	0.991	0.995	0.998

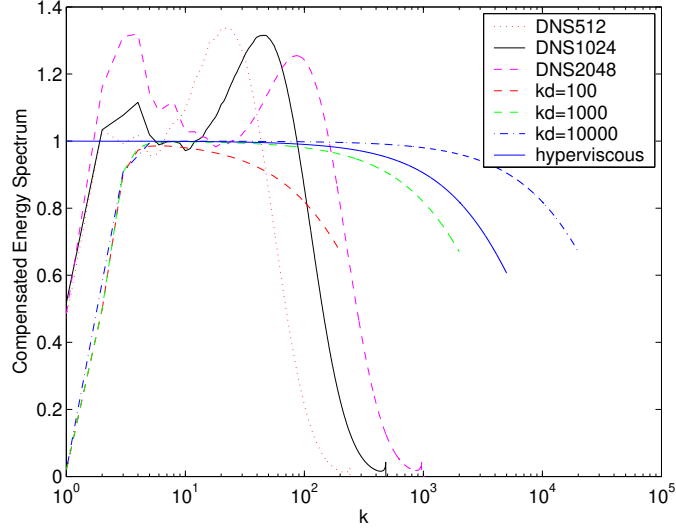


Figure 1: The compensated energy spectra $E^*(k) = E(k)k^{5/3} = K_k \circ$ vs. k for realistic turbulent flow [Eq. (7)] with $(k_d; \circ) = (100; 0.2); (1000; 0.2); (10000; 0.2); (10000; 1)$, and from numerical simulations on $512^3; 1024^3$ and 2048^3 grids. $c = 1.0$ and $c = 0.2$ correspond to hyperviscosity and ordinary viscosity respectively.

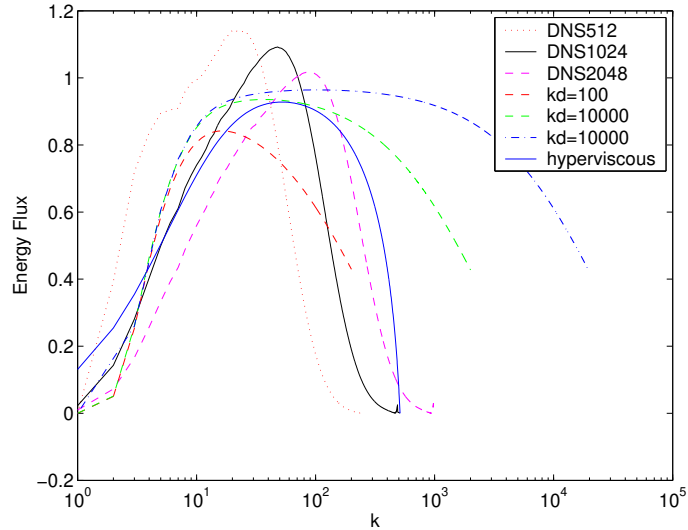


Figure 2: The computed flux (k_0) using Eq. (5) for realistic turbulent flow [Eq. (7)] with $(k_d; \circ) = (100; 0.2); (1000; 0.2); (10000; 0.2); (10000; 1)$, and from numerical simulations on $512^3; 1024^3$ and 2048^3 grids.

Figures